Coupling between the Thermal Evolution of the Heme Pocket and the External Matrix Structure in *Trehalose Coated* Carboxymyoglobin

Sergio Giuffrida, Grazia Cottone, Fabio Librizzi, and Lorenzo Cordone*

Istituto Nazionale di Fisica della Materia, Dipartimento di Scienze Fisiche ed Astronomiche, Universitá di Palermo, Via Archirafi 36, I-90123 Palermo, Italy

Received: July 28, 2003; In Final Form: September 18, 2003

Proteins can assume a very large number of conformations (conformational substates), all concurring to its function. We present experimental evidence for the existence, in *trehalose coated* carboxymyoglobin, of a structured environment of the protein, tightly coupled to the heme pocket structure, as experienced by the bound CO molecule. This was evidenced by the strict correlation observed between the thermal evolution (300−20 K) of the CO stretching and of the water association bands in samples of carboxymyoglobin embedded in trehalose matrixes of different hydration. This observation put forward the coupling between the degrees of freedom of the matrix and those of the protein. In the driest sample, in which only tightly bound, nonremovable water molecules were present, temperature induced structural variations of both the heme pocket and the external matrix were small, even at room temperature. At variance, such variations were larger in two water richer samples in which their onset was already at ∼50 K. Further, the thermal evolution of the CO stretching and of the water association bands showed a single linear correlation for the drier samples in the whole temperature range investigated. The same correlation was observed for the water richest sample up to ∼180 K, that is, the temperature at which a dynamic transition for the protein motions has been recurrently observed by experimental and computational means, in water containing systems. The data presented enable us to suggest the existence of a rigid water dipole network, which extends throughout the sample, impeding structural heme pocket rearrangements, which imply charge displacement. This in turn brings about the lack of thermally induced variations of the stretching band of the bound CO, which reflects the distribution of taxonomic (A) and lower tier conformational substates. Accordingly, in agreement with previous suggestions, we speculate that, in solution, slaving of the protein internal dynamics to the dynamics of the external solvent is brought about by the "attempts" of the protein structure to match the rapidly evolving structure of the water dipole network.

1. Introduction

Biological structures embedded in sugar matrixes can overcome adverse conditions such as dehydration and/or high temperatures. In particular, trehalose (a disaccharide composed of two [1,1]-linked α,α units of glucopyranose) appears as the most effective protectant in terms of functional recovery and reutilization of biomaterials after drying and resuspension.[1−5] This sugar is present in some organisms that can survive lack of water and high temperature without suffering damage, under a condition known as *anhydrobiosis*. These organisms can remain in anhydrobiosis for several years, while, upon rehydration, their vegetative cycles restart.

The dynamic behavior of *saccharide coated* proteins has been extensively studied.[6−12] Cordone et al.[13] reported that in *trehalose coated* carboxymyoglobin (MbCO) the quasi-diffusive (nonharmonic) motions of the iron atom, which in hydrated samples appear above ∼180 K,[14] are severely hindered even at room temperature. Large hindering was also reported for the nonharmonic contributions to the hydrogen atoms' mean square displacement.[15] Moreover, reduction of the nonharmonic contributions to motions, for all classes of atoms, was obtained in a molecular dynamics simulation on a system containing one MbCO molecule embedded in a 89% w/w trehalose/water matrix.[16]

As it is well-known, the stretching band of the bound CO in MbCO (see Figure 1) is split into three different sub-bands reflecting the taxonomic (A) substates,[17] which correspond to three specific different environments experienced by the bound CO within the heme pocket.[18] The areas under these sub-bands, which reflect the relative populations of the three conformers (A substates), depend on external parameters such pH, temperature, and pressure.[18−21] The thermal behavior of such sub-bands, therefore, conveys information on the heme pocket structural evolution, which is reflected in the thermal evolution of the shape of the CO stretching band.

As shown in Figure 1, on the high frequency side of the CO stretching band there appears the water association band. This band, which is absent in water vapors, is attributed[22] to a combination of the bending mode of water molecules with intermolecular vibrational modes. The band (see Figure 2a) is not structured in pure water, while it is sizably structured in trehalose dihydrate powders (see Figure 2b). Due to the rapid water uptake during the transfer to the apparatus for FTIR measurements on powder, we did not succeed in performing FTIR measurements in fully anhydrous trehalose powders. To ascertain whether sugar components contribute to the band, we measured the FTIR spectrum of a sample of anhydrous sucrose powder (see Figure 2c). On the basis of the very low absorption observed in such sample, we inferred that the band must be absent also in anhydrous trehalose. We mention that, following

* Corresponding author. E-mail: cordone@fisica.unipa.it.

10.1021/jp036194x CCC: $25.00
Published on Web 10/31/2003

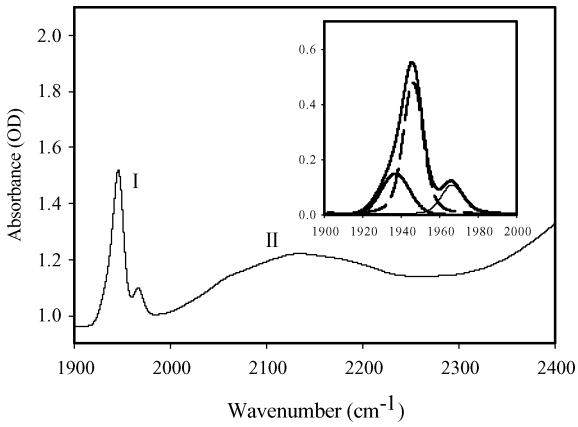

Figure 1. CO stretching band (I, 1900−2000 cm^{-1}) and association band of water (II, 2000−2400 cm^{-1}) in trehalose coated MbCO. The inset shows the fitting of the CO band in terms of three taxonomic A substates.[17] Data refer to sample #3, at $T = 300$ K.

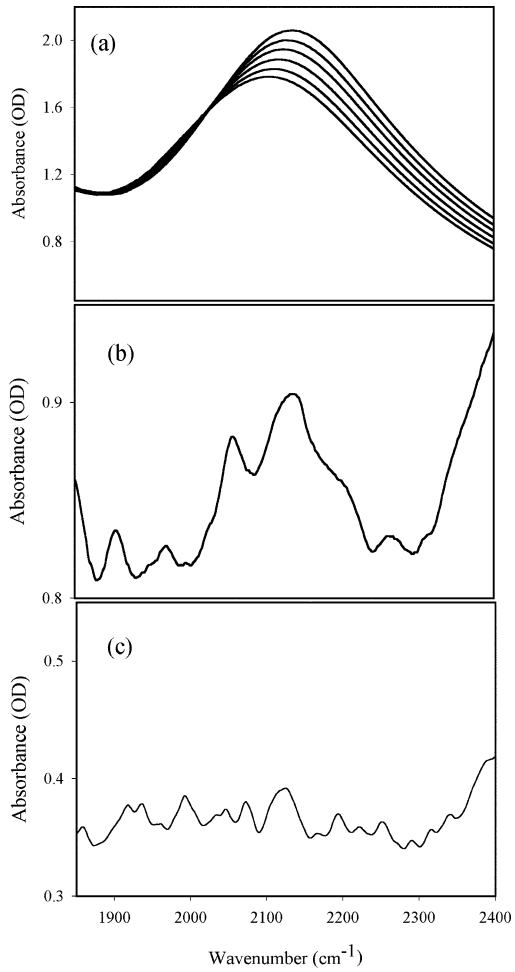

Figure 2. (a) Water association band in pure water, in the temperature range 280−330 K; (b) water association band in dihydrate trehalose powders, at room temperature; (c) absorption profile of anhydrous sucrose powders in the range 2000−2400 cm^{-1}, at room temperature.

a short exposure of the above anhydrous crystalline sucrose sample to moisture, a water band appears, whose structure is sizably different from that of the band in Figure 2b (data not shown). In view of the above observation and of the scarce water−water interaction in trehalose dihydrate powder, we suggest that the structured band in Figure 2b does not only arise from direct coupling among water molecules. Coupling of the bending modes of water molecules with intermolecular vibrational modes involving non-water OH groups should also contribute to the band. This should hold true also for the bands of the plasticized amorphous or glassy samples of trehalose coated MbCO, below reported. The area under the water association band has been used for estimating the rate of water release when drying samples of MbCO either trehalose coated or in the absence of trehalose[23] under dry nitrogen flux.

Librizzi et al.[24] studied the relation between the protein internal dynamics and the dynamics of the external matrix, in *trehalose coated* MbCO. To this purpose, the authors analyzed the thermal behavior of the CO and water association bands in the temperature range 263−323 K and the room-temperature kinetics of CO rebinding; the measurements were performed using samples of different water content, which was estimated through the area under the water association band. In the present work we extended the FTIR study to a larger temperature interval (300−20 K). We obtained information on the structural evolution of the protein, in the vicinity of the heme pocket, and of the external matrix, by plotting, for both the CO stretching and water association bands, the spectral distance (SD) of the various normalized spectra from the respective normalized spectrum measured at 20 K.

This is defined as[25]

$$\mathrm{SD} = \left\{ \sum_{\nu} [A(\nu,T) - A(\nu,T = 20\ \mathrm{K})]^{2} \Delta\nu \right\}^{1/2}$$

where $A(\nu)$ is the normalized absorbance at frequency ν and $\Delta\nu$ is the frequency resolution. The above quantity represents the deviation of the normalized spectrum at temperature T from the normalized spectrum at 20 K; for the protein it reflects the overall thermally induced heme pocket structural changes evidenced by the changes in the population of taxonomic (A) and lower hierarchy substates. In view of the structured profile of the water association band (see below), we assumed that, for this band, SD reflects thermally induced structural rearrangements of the water molecules' network within our samples either solid or plasticized amorphous. This assumption will appear, a posteriori, well justified.

2. Materials and Methods

Lyophilized ferric horse myoglobin was purchased from Sigma (Sigma, St. Louis, MO) and used without further purification. Trehalose from Hayashibara Shoij (Hayashibara Shoij Inc., Okayama, Japan) was used after recrystallization from aqueous solutions. For sample preparation, myoglobin was dissolved ($\sim 5 \times 10^{-3}$ M) in a solution containing 2×10^{-1} M trehalose and 2×10^{-2} M phosphate buffer (pH 7 in water). The solution was equilibrated with CO and reduced by anaerobic addition of sodium dithionite (10^{-1} M). Aliquots (0.1 mL) of the above solution were layered on CaF_2 windows of an ~ 1 cm^2 surface. All samples were initially dried for about 8 h under a CO atmosphere in a silica gel desiccator. Further drying proceeded at 353 K: 1 h at ambient pressure and about 15 h under vacuum. Samples containing various amounts of residual water were then prepared as follows:

(I) The driest sample studied (#1) was—after drying at 353 K—immediately put into the sample holder and transferred into the cryostat where it was left *open* to allow further drying under vacuum ($\sim$1.5 h at 353 K), getting rid of the traces of water adsorbed when mounting the sample on the holder. Measurements were then performed in the temperature interval 350−20 K. This hard and glassy sample still contained traces of tightly bound, not removable, water (see below).

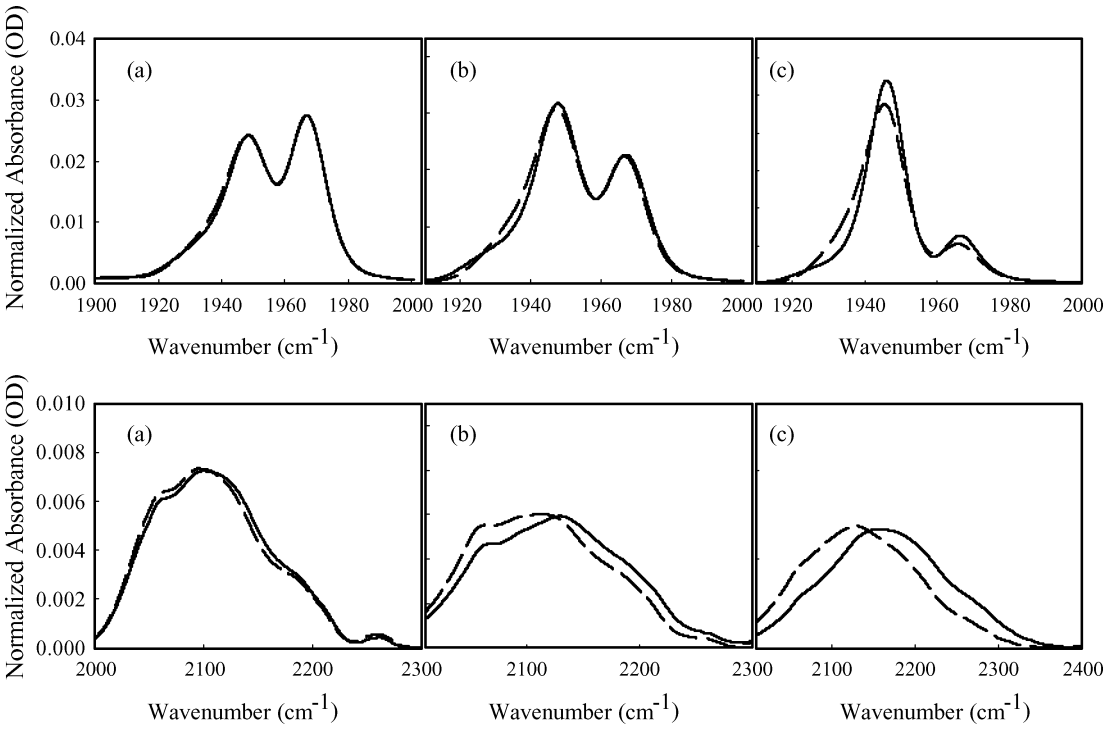

Figure 3. Normalized spectra of the CO stretching band (upper panels) and of the water association band (lower panels) at 20 K (solid lines) and 300 K (dashed lines): (a) sample #1; (b) sample #2; (c) sample #3. Results are very well reproducible, within a few percent.

(II) A second sample (#2) was—after drying at 353 K—exposed for ∼3 min to room moisture at 300 K, before putting it into the sample holder. This allowed slight water uptake. The sample was then confined by putting a Teflon O-ring and a second CaF_2 window on top of it, to avoid water release during measurements, and transferred into the cryostat where it was left for ∼2 h, at room temperature, before starting measurements. This allowed diffusion of the absorbed water. Measurements were then performed in the temperature interval 300−20 K.

(III) A further sample (#3) was—after drying at 353 K—overnight equilibrated in the presence of 60% relative humidity at 300 K. The sample was then put into the holder and confined by putting a Teflon O-ring and a second CaF_2 window on top of it, to avoid water evaporation, and then transferred into the cryostat. Measurements were performed in the temperature interval 300−20 K. After hydration the sample was not dipping and remained hard enough to stay in a vertical position.

(IV) A control sample (#4), not containing protein, was also measured. The sample was prepared in such a way as to have about the same overall mass (trehalose + protein) as the protein containing ones. Accordingly, we prepared a solution containing 4×10^{-1} M trehalose and 2×10^{-2} M phosphate buffer (pH 7 in water). This solution was equilibrated with CO before adding 10^{-1} M sodium dithionite. A 0.1 mL aliquot of the above solution was layered on CaF_2 windows of an ∼1 cm^2 surface. The sample was then dried following exactly the same procedure as that for sample #1. We stress that the drying of the sample ended only when no further decrease of the water association band was observed by further leaving the sample (2 h) under vacuum at 353 K.

After the above treatments, all samples remained in an amorphous state. This was also evidenced by the very low turbidity detected by measuring the absorbance at 1900 cm^{-1} at 300 K.[23] Moreover, as reported for samples that underwent similar treatment,[15] the myoglobin molecule could be fully recovered. This is also put forward by the fact that water uptake, by the overdried sample, makes the shape of the CO band evolve toward the one of a nontreated protein in aqueous solution (see below and Figure 3, upper panels).

A very rough and qualitative estimate of the samples' water content was obtained by measuring, in o.d. × cm^{-1}, the overall area under the profile of the association band at 300 K. The measured areas were 5.5 and 7.2 o.d. × cm^{-1} for samples #1 and #2, respectively, 31.5 o.d. × cm^{-1} for the humidified sample #3, and 12.7 o.d. × cm^{-1} for the control sample #4. Note that in order to compare data referring to analogous masses of trehalose, we divided the area measured for sample #4 (25.4 o.d. × cm^{-1}) by a of factor 2. The data seem to indicate that, in overdried samples, the presence of the protein makes the water content decrease with respect to that for pure trehalose glasses. We are presently performing gravimetric measurements in order to get detailed information on this effect.

We also estimated the water content in the samples by exploiting the intermolecular water band at ∼5200 cm^{-1}, which is ascribed to a combination of bending with asymmetric stretching.[22] This band was recently used to estimate the water content in samples of trehalose coated photosynthetic reaction centers.[26,27] This estimate was 0.24, 1.15, and 18 o.d. × cm^{-1} for samples #1 to #3, respectively, and 1.5o.d. cm^{-1} for sample #4; also, in this case, the overall measured area for the last sample was divided by a of factor 2. As it is evident, although the two estimates are in qualitative agreement, the correlation between the two measurements is not linear. We ascribe this behavior to different effects of trehalose coating and extreme drying on the oscillator strength of the different bands. In this respect we note that, in our samples, the water association band shows a structure. This structure stems from the presence of different sub-bands, having different oscillator strengths, whose relative weight varies upon drying. We stress, however, that we are not interested in the detailed water content but rather in roughly and qualitatively estimating differences between samples.

All FTIR measurements were performed on a Jasco 410 FTIR spectrometer with 2 cm^{-1} resolution. The cryostat and the

temperature controller used were respectively Optistat CF-V and ITC-503, both from Oxford Instruments Ltd., U.K.

The CO band (1900−2000 cm^{-1}) was fitted in terms of the three A substates.[17] A Gaussian extrapolation took into account the queue of the association band in the range 1900−2000 cm^{-1}. The fitting of the water association band was performed in terms of Gaussian and/or voigtian components, which were dependent on the sample humidity. The details and the thermal evolution of the above sub-bands will be discussed elsewhere. A Gaussian extrapolation took into account the queue of the adjacent higher frequency bands (ν > 2400 cm^{-1}). The above fitting gave the areas under the absorption profiles that were used for normalization of the raw data.

3. Results and Discussion

The bands of CO stretching at 20 and 300 K, as obtained after extraction from the raw data and normalization, are shown in Figure 3 (upper panels). We are dealing with normalized spectra, as we are interested in changes of the absorption profile that reflect heme pocket conformational rearrangements. It must be considered, however, that the temperature dependence of the area under the CO band is very limited; indeed, the overall area under the band only varies by a mere 1% in the whole temperature interval. As it is evident, much smaller temperature induced profile variations take place in the very dry sample #1 with respect to samples #2 and #3.

Normalized absorption profiles of the water association band at 20 and 300 K, as obtained after extraction from the raw data and normalization, are shown in the lower panels of Figure 3. Due to the origin of the band, the non-normalized areas under the absorption profile have a large temperature dependence, brought about by the temperature variation of the relative distance among the interacting molecules. Once more, we are dealing with normalized spectra, as we are interested in variations of the band profile that contain information on the structural rearrangements of the water dipoles in the network.

Figure 4 show the spectral distances (see eq 1) of the CO stretching and of the water association bands (respectively, SD_{CO} and SD_{WATER}), referred to the spectrum at 20 K. The figure better evidences the small temperature dependence of the profiles of the CO and of the water bands in the very dry sample #1, as compared to samples #2 and #3. In particular, in the last two samples the SDs are already temperature dependent at ∼50 K; moreover, they are almost coincident up to ∼180 K, while at a higher temperature the water richest sample #3 exhibits a larger increase than sample #2. As mentioned above, SDs relative to the CO stretching band convey condensed information on the thermal evolution of the heme pocket structure as experienced by the bound CO, while SDs relative to the water band convey condensed information on the thermal evolution of the matrix structure, as experienced by the water molecules. Accordingly, a comparison of data in parts a and b of Figure 4 puts forward the strict structural coupling between the heme pocket and the external matrix.

Rector et al.[11] suggested that structural fluctuations involving displacement of the protein surface can take place even in highly viscous fluids but are severely hindered when the protein surface topology is fixed in a solid trehalose glass. As a matter of fact, since the solid solvent resists any shearing motion, the surface of the protein can only change by elastic distortions of the external matrix. Moreover, due to the extremely low compressibility of the solid glass, only such fluctuations are permitted as do not move the protein surface very far. Librizzi et al.[24] studied the thermal behavior of the CO stretching in the

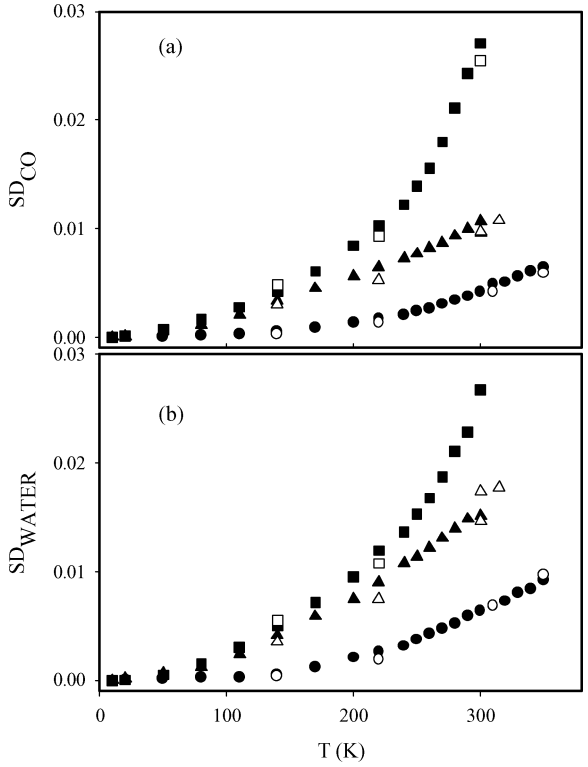

Figure 4. (a) CO stretching band spectral distance (SD_{CO}) referred to the spectrum measured at 20 K vs temperature. (b) Water association band spectral distance (SD_{WATER}) referred to the spectrum measured at 20 K vs temperature: circles, sample #1; triangles, sample #2; squares, sample #3; full symbols, data points obtained during cooling; open symbols, data points obtained during heating. The very good reproducibility of the data points indicates that we are dealing with systems in thermal equilibrium. As evident in samples #2 and #3, low temperature interconversion among suitable low hierarchy conformational substates takes place already at 50 K, both in the protein and in the matrix.

temperature range 263−323 K, and the room temperature CO recombination after flash photolysis, in trehalose coated MbCO samples of different hydration, similar to the ones presently studied. On the basis of the data reported by Rector et al.,[11] the authors concluded that in the dry trehalose samples, similar to samples #1 and #2, the temperature induced variations of the heme pocket structure essentially are internal processes not involving displacements of the protein surface. At variance, such displacements can take place, in the temperature range they explored, following exposure of the sample to 60% relative humidity.

According to Librizzi et al.,[24] the data in Figure 4 (SDs) can therefore be interpreted by considering the following:

(i) In the whole temperature range investigated, samples #1 and #2 are solid glasses in which the thermal behavior of SD_{CO} arises from protein internal processes, which involve low hierarchy substates and take place without displacement of the protein surface.

(ii) At variance, sample #3 is a solid glass, in which processes not involving displacements of the protein surface take place, only in the temperature interval 20−180 K. At higher temperatures, that is, above the glass transition temperature (which according our data should be ∼180 K), the sample becomes a plasticized amorphous sample in which structural rearrangements of the protein are accompanied by surface displacement.[24,26] The plot in Figure 5 further confirms this suggestion.

To get closer information on the correlation between the thermal evolution of the protein and the thermal evolution of

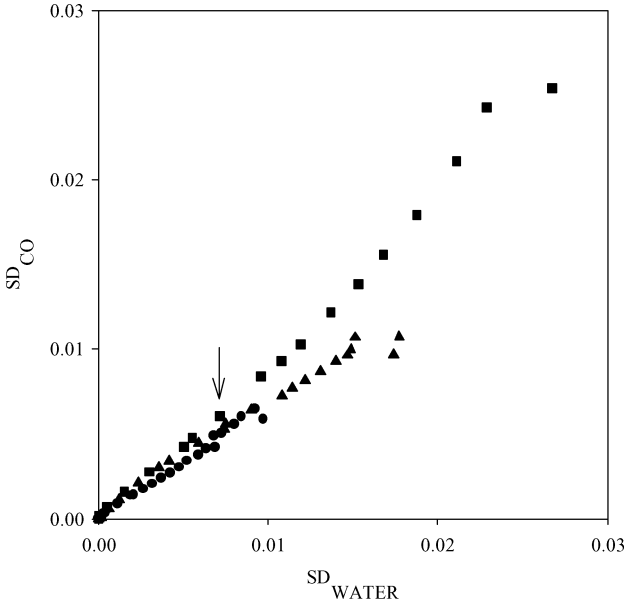

Figure 5. Plot of the SD_{CO} vs the SD_{WATER}: circles, sample #1; triangles, sample #2; squares, sample #3. The arrow indicates the point corresponding to $T \sim 180$ K for samples #2 and #3.

the external matrix structures, we plotted (see Figure 5) SD_{CO} as a function of SD_{WATER}. As Figure 5 shows, the evolution of the structure of the protein and of the external matrix exhibits a single linear correlation, almost independent of water content, for samples #1 and #2 in the whole temperature range investigated. At variance, a deviation is evident for the humid sample #3, which becomes sizable at ~180 K, that is, the temperature above which (see Figure 4) the SD of sample #3 starts exhibiting larger values than the SD of sample #2.

On the basis of the above two points (i and ii) and on the data in Figure 5, we suggest that the thermal evolution of the protein structure is fully slaved to the thermal evolution of the overall trehalose/water matrix structure, in the whole temperature range for samples #1 and #2. At variance, for sample #3 such full slaving takes place only in the temperature interval 20−180 K.

It has recently been reported[28] that, in trehalose/water/protein systems, structures are formed that contain trehalose molecules, mainly bound to the protein through single hydrogen bonds, and water molecules in excess over their concentration in the bulk solvent. In such structures the myoglobin molecule is confined within a network of hydrogen bonds connecting protein groups, water molecules, and trehalose molecules. Moreover, the fraction of water molecules forming multiple hydrogen bonds with both protein and sugar was found to increase by decreasing the water content. Since the water motional freedom decreases by increasing the number of hydrogen bonds in which each molecule is involved, one expects the water dipole network to exhibit decreasing temperature induced rearrangements, when reducing the content of residual water.[24,26] In turn, according to the suggestion that the structural relaxation of a protein is coupled to the relaxation of the hydrogen bond network,[29] this should be reflected in a decrease of the protein structural variations, when the water content is decreased.

In line with suggestions by Cottone et al.,[28] the present results show that sample #1, whose water molecules are not removable even after prolonged drying at 363 K under vacuum, behaves as a solid glass at all temperatures. In this sample thermally induced structural changes of the protein and of the external matrix are extremely reduced. In sample #2, which contains

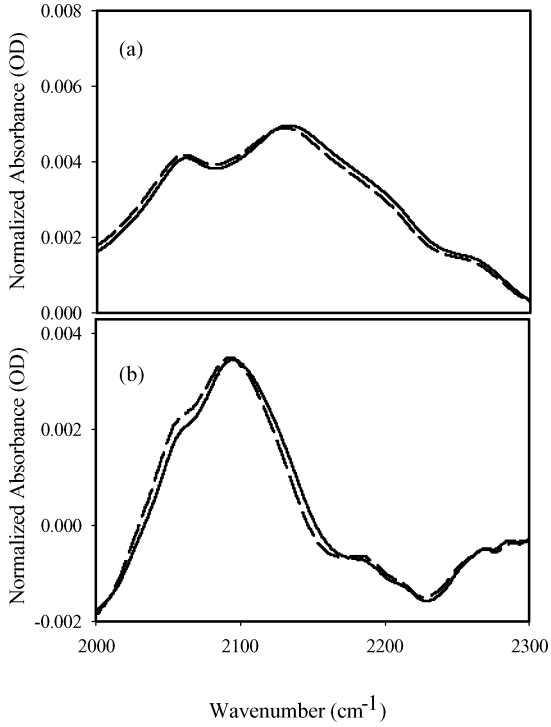

Figure 6. (a) Normalized spectra of the water association band in the control sample #4, at 20 K (solid line) and at 300 K (dashed line). Note the sizable shape difference with respect to the spectrum of crystalline dihydrate in Figure 2b. (b) Difference between the spectra of the water association band in trehalose coated MbCO sample #1 and in sample #4, at 20 K (solid line) and at 300 K (dashed line).

water molecules that can be removed by drying at 353 K under vacuum, the structural variations of both the external matrix and the protein are slightly larger than those in sample #1. However, as previously mentioned, also this sample behaves as a solid glass. Accordingly, the correlated behavior of SD_{CO} and SD_{WATER} in samples #1 and #2 is indicative of a long-range and long-lived structural correlation. We believe this to be brought about by the propagation of the recently observed[30] solvent structures at the protein surface over the whole sample.

In Figure 6a we report the normalized FTIR spectrum of the control sample #4 at 20 and 300 K. A comparison of Figure 2b with Figure 6 shows that the structure of the spectrum of the glassy sample in Figure 6a is largely different from the structure of the spectrum of the crystalline dihydrate powder shown in Figure 2b. Sample #4 does not undergo crystallization either after prolonged storage or after cycling the temperature. We did not perform measurements in samples—not containing protein—of larger water content, since crystallization occurred either during storage or during measurements, due to water mobility. We think it worth mentioning that no crystallization occurred in protein containing samples during our measurements.

Figure 6b shows the difference between the normalized spectrum of sample #1 and the normalized spectrum of sample #4. As it is evident, as a counterpart of the effects that the trehalose matrix has on the structure of the embedded protein, the presence of the protein influences the structure of the trehalose/water matrix. Furthermore, in Figure 7 we show the SD_{WATER} relative to sample #4, superimposed, for the sake of comparison, to the SD_{WATER} relative to sample #1, already reported in Figure 4b. As the figure shows, in the absence of the protein, the thermally induced structural variations of the water/trehalose matrix are lower than those in the protein containing sample, notwithstanding the larger water content of

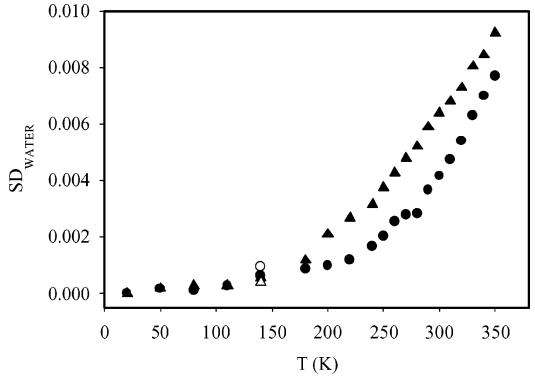

Figure 7. Water association band spectral distance (SD_{WATER}) for samples #4 (circles) and #1 (triangles): full symbols, data points obtained during cooling; open symbols, data points obtained during heating.

the former. This is indicative, in dry samples, of a reciprocal protein ↔ matrix full structural slaving over the whole temperature range explored and that the presence of the embedded protein must play a relevant role on the glass transition temperature of protein containing samples. Accordingly, samples #1 and #2 behave as solid systems whose structure and dynamics are governed by a single hierarchically organized energy landscape defined in a $3N - 3$ space, where N is the total number of atoms present in the sample. In particular, different matrix and protein structures are observed when MbCO is embedded in matrixes of different saccharides (work in progress).

As Figures 4 and 5 show, the SD values for samples #2 and #3 are similar up to ∼180 K, becoming larger for the last at higher temperatures. According to Cottone et al.,[28] this behavior is conceivably due to the different water contents between the two samples. In fact, weakly bound, *bulklike*[31] water molecules present in this sample above ∼180 K break the protein/matrix long-range structural (and dynamic) correlation. In this respect we note that ∼180 K is, recurrently, the temperature at which the so-called dynamic transition has been observed in experimental and simulative studies, in protein/water systems.[14,30,32−33] This behavior implies that, in nonsolid systems, the $3N - 3$ space in which the above energy landscape is defined includes only the atoms tightly interacting with the protein, which in solution essentially include the atoms in the protein hydration shell.[34]

4. Conclusions

Slaving of the internal dynamics of a protein to the dynamics of the external solvent is long standing and well established.[35−38] The present results give evidence for a tight coupling between the degrees of freedom of the matrix and those of the protein. In hard matrixes the protein/matrix structural coupling is long-lived and long-range, extending through the whole sample. At variance, by softening the external matrix, it gradually becomes short-lived and short-range, in view of the rapid and uncorrelated flickering of hydrogen bond networks. It has been suggested that the solvent injects its dynamics into the macromolecule through the continuous forming and breaking of hydrogen bonds involving the solvent exposed lateral chains[39−44] and that the solvent dielectric fluctuations (which involve fluctuation of the water dipole structure) mostly drive the slaving process.[38] In full agreement, our data indicate that under conditions in which the water dipole network is rigid and "*not flickering*", as in dry trehalose systems or at low temperature, the thermally induced heme pocket rearrangements are hindered, as is the consequent redistribution of taxonomic (A) and lower tier conformational substates. On the basis of these results, we speculate that, in aqueous solution, slaving of the protein internal dynamics to the dynamics of the external solvent is due to the "*attempts*" of the protein structure to "*match*" the flickering structure of the water dipole network.

An intriguing point arises when considering the strong similarity between the plot of SD_{CO} vs T (see Figure 4a) and analogous plots in which are reported the iron atom mean square displacements measured in the $\sim 10^{-7}$ s time scale by Mössbauer spectroscopy[13,14] or the hydrogen atoms' mean square displacements, in the $\sim 10^{-10}$ to 10^{-9} s time scale, measured by elastic neutron scattering.[15,32,45] Such a comparison evidences that the thermal evolution of equilibrium structures (conformational substates), obtained by FTIR, strictly parallels the thermal evolution of mean square displacements of different atoms, measured on different time scales. This unambiguously shows that the amplitude increase of the mean square fluctuations, which takes place above ∼180 K, stems from interconversion among high hierarchy conformational substates, as up to now assumed. Work is in progress to put this last point on a quantitative ground.

Acknowledgment. We thank M. B. Vittorelli and M. U. Palma for useful discussions and criticisms. This work is part of a project cofinanced by MIUR (Ministero dell'Istruzione, dell'Università e della Ricerca) ex MURST and by the European Community (European Funds for Regional Development). Partial support has also been obtained from MIUR project Cofin 2000.

References and Notes

(1) Crowe, J. H.; Crowe, L. M. *Science* **1984**, *223*, 701−703.
(2) Crowe, L. M.; Crowe, J. H. In *Liposomes, New systems and new trends in their applications*; Puisieux, F., Covreur, P., Delattre, L., Devissaguet, J. P., Eds.; Editions de Santè: Paris, 1995; pp 237−272.
(3) Bianchi, G.; Gamba, A.; Murellie, C.; Salamini, F.; Bartels, D. *Craterostigma Plantagineum. Plant J.* **1991**, *1*, 355−359.
(4) Uritani, M.; Takai, M.; Yoshinaga, K. *J. Biochem.* **1995**, *117*, 774−779.
(5) Panek, A. D. *Braz. J. Med. Biol. Res.* **1995**, *28*, 169−181.
(6) Hagen, S. J.; Hofrichter, J.; Eaton, W. A. *Science* **1995**, *269*, 959−962.
(7) Hagen, S. J.; Hofrichter, J.; Eaton, W. A. *J. Phys. Chem.* **1996**, *100*, 12008−12021.
(8) Gottfried, D. S.; Peterson, E. S.; Sheikh, A. G.; Wang, J.; Yang, M.; Friedman, J. M. *J. Phys. Chem.* **1996**, *100*, 12034−12042.
(9) Kleinert, T.; Doster, W.; Leyser, H.; Petry, W.; Schwarz, V.; Settles, M. *Biochemistry* **1998**, *37*, 717−733.
(10) Lichtenegger, H.; Doster, W.; Kleinert, T.; Birk, A.; Sepiol, B.; Vogl, G. *Biophys. J.* **1999**, *76*, 414−422.
(11) Rector, D.; Jiang, J.; Berg, M. A.; Fayer, M. D. *J. Phys. Chem. B* **2001**, *105*, 1081−1092.
(12) Dantsker, D.; Samuni, U.; Friedman, A. J.; Yang, M.; Ray, A.; Friedman, J. M. *J. Mol. Biol.* **2002**, *315*, 239−251.
(13) Cordone, L.; Galajda, P.; Vitrano, E.; Gassmann, A.; Ostermann, A.; Parak, F. *Eur. Biophys. J.* **1998**, *27*, 173−176.
(14) Parak, F.; Knapp, E. W.; Kucheida, D. *J. Mol. Biol.* **1982**, *161*, 177−194.
(15) Cordone, L.; Ferrand, M.; Vitrano, E.; Zaccai, G. *Biophys. J.* **1999**, *76*, 1043−1047.
(16) Cottone, G.; Cordone, L.; Ciccotti, G. *Biophys. J.* **2001**, *80*, 931−938.
(17) Frauenfelder, H.; Parak, F.; Young, R. D. *Annu. Rev. Biophys. Chem.* **1988**, *17*, 451−479.
(18) Vojtechovsky, J.; Chu, K.; Berendzen, J.; Sweet, R. M.; Schlichting, I. *Biophys. J.* **1999**, *77*, 2153−2174.
(19) Makinen, M. W.; Houtchens, R. A.; Caughey, W. S. *Proc. Natl. Acad. Sci. U.S.A.* **1979**, *76*, 6042−6046.
(20) Beece, D.; Eisenstein, L.; Frauenfelder, H.; Good, D.; Marden, M. C.; Reinisch, L.; Reynolds, A. H.; Sorensen, L. B.; Yue, K. T. *Biochemistry* **1980**, *19*, 5147−5157.
(21) Frauenfelder, H.; Alberding, N. A.; Ansari, A.; Braunstein, D.; Cowen, B. R.; Hong, M. K.; Iben, I. E. T.; Johnson, J. B.; Luck, S.; et al. *J. Phys. Chem.* **1990**, *94*, 1024−1037.

(22) Eisenberg, D.; Kauzmann, W. *The Structure and Properties of Water*; Oxford University Press: London, 1969.
(23) Librizzi, F.; Vitrano, E.; Cordone, L. *Biophys. J.* **1999**, *76*, 2727−2734.
(24) Librizzi, F.; Viappiani, C.; Abbruzzetti, S.; Cordone, L. *J. Chem. Phys.* **2002**, *116*, 1193−1200.
(25) The expression within braces in eq 1 is the discrete approximation of the integral $\int_\nu [A(\nu,T) - A(\nu,T=20\ \mathrm{K})]^2\, d\nu$.
(26) Palazzo, G.; Mallardi, A.; Hochkoeppler, A.; Cordone, L.; Venturoli, G. *Biophys. J.* **2002**, *82*, 558−568.
(27) Francia, F.; Palazzo, G.; Mallardi, A.; Cordone, L.; Venturoli, G. *Biophys. J.* **2003**, *85*, 2760−2775.
(28) Cottone, G.; Ciccotti, G.; Cordone, L. *J. Chem. Phys.* **2002**, *117*, 9862−9866.
(29) Tarek, M.; Tobias, D. J. *Phys. Rev. Lett.* **2002**, *88*, 8101−8104.
(30) Teeter, M. M.; Yamano, A.; Stec, B.; Mohanty, U. *Proc. Natl. Acad. Sci. U.S.A.* **2001**, *98*, 11242−11247.
(31) Pal, S. K.; Peon, J.; Zewail, A. H. *Proc. Natl. Acad. Sci. U.S.A.* **2002**, *99*, 1763−1768.
(32) Doster, W.; Cusak, S.; Petry, W. *Nature* **1989**, *337*, 754−756.
(33) Steinbach, P. J.; Loncharich, R. J.; Brooks, B. R. *Chem. Phys.* **1991**, *158*, 383−394.
(34) Frauenfelder, H.; Fenimore, P. W.; McMahon, B. H. *Biophys. Chem.* **2002**, *98*, 35−48.
(35) Ansari, A.; Berendzen, J.; Braunstein, D.; Cowen, B. R.; Frauenfelder, H.; Hong, M. K.; Iben, I. E. T.; Johnson, J. B.; Ormos, P.; Sauke, T. B.; et al. *Biophys. Chem.* **1987**, *26*, 337−355.
(36) Réat, V.; Dunn, R.; Ferrand, M.; Finney, J. L.; Daniel, R. M.; Smith, J. C. *Proc. Natl. Acad. Sci. U.S.A.* **2000**, *97*, 9961−9966.
(37) Vitkup, D.; Ringe, D.; Petsko, G. A.; Karplus, M. *Nat. Struct. Biol.* **2000**, *7*, 34−38.
(38) Fenimore, P. W.; Frauenfelder, H.; McMahon, B. H.; Parak, F. *Proc. Natl. Acad. Sci. U.S.A.* **2002**, *99*, 16047−16051.
(39) Bizzarri, A. R.; Cannistraro, S. *J. Phys. Chem. B* **2002**, *106*, 6617−6633.
(40) Careri, G. In *Biological Physics*; Frauenfelder, H., Hummer, G., Garcia, R., Eds.; AIP American Institute of Physics: Melville, NY, 1999; pp 8−13.
(41) Doster, W.; Bacheitner, A.; Dunau, R.; Hiebl, M.; Luscher, E. *Biophys. J.* **1986**, *50*, 213−219.
(42) Green, J. L.; Fan, J.; Angell, C. A. *J. Phys. Chem.* **1994**, *98*, 13780−13790.
(43) Goldanskii, V. I.; Krupyanskii, Y. F. *Q. Rev. Biophys.* **1989**, *22*, 39−92.
(44) Barron, L. D.; Hecht, L.; Wilson, G. *Biochemistry* **1997**, *36*, 13143−13147.
(45) Librizzi, F.; Paciaroni, A.; Pfister, C.; Vitrano, E.; Zaccai, G.; Cordone, L. In *Proceedings of ILL Millenium Symposium and European User Meeting*; 2001; pp 58−59.